Biophysical Journal
Article

Biophysical Society

Facilitated dissociation of nucleoid-associated proteins from DNA in the bacterial confinement

Zafer Koşar,[1] A. Göktuğ Attar,[1,2] and Aykut Erbaş[1,*]
[1]UNAM-National Nanotechnology Research Center and Institute of Materials Science & Nanotechnology, Bilkent University, Ankara, Turkey and [2]Department of Molecular Biology & Genetics, Bilkent University, Ankara, Turkey

ABSTRACT Transcription machinery depends on the temporal formation of protein-DNA complexes. Recent experiments demonstrated that not only the formation but also the lifetime of such complexes can affect the transcriptional machinery. In parallel, in vitro single-molecule studies showed that nucleoid-associated proteins (NAPs) leave the DNA rapidly as the bulk concentration of the protein increases via facilitated dissociation (FD). Nevertheless, whether such a concentration-dependent mechanism is functional in a bacterial cell, in which NAP levels and the 3d chromosomal structure are often coupled, is not clear a priori. Here, by using extensive coarse-grained molecular simulations, we model the unbinding of specific and nonspecific dimeric NAPs from a high-molecular-weight circular DNA molecule in a cylindrical structure mimicking the cellular confinement of a bacterial chromosome. Our simulations confirm that physiologically relevant peak protein levels (tens of micromolar) lead to highly compact chromosomal structures. This compaction results in rapid off rates (shorter DNA residence times) for specifically DNA-binding NAPs, such as the factor for inversion stimulation, which mostly dissociate via a segmental jump mechanism. Contrarily, for nonspecific NAPs, which are more prone to leave their binding sites via 1d sliding, the off rates decrease as the protein levels increase. The simulations with restrained chromosome models reveal that chromosome compaction is in favor of faster dissociation but only for specific proteins, and nonspecific proteins are not affected by the chromosome compaction. Overall, our results suggest that the cellular concentration level of a structural DNA-binding protein can be highly intermingled with its DNA residence time.

SIGNIFICANCE Vital cellular processes such as transcription rely on the formation of temporary protein-DNA complexes. Until recently, disassembly of these complexes was thought to be a random process. However, recent studies show that a protein's bulk concentration impacts the stability of its complexes with DNA. Yet, for nucleoid-associated proteins, the 3d genome organization and protein levels are also coupled, suggesting a complicated relationship between the cellular level of a structural protein, its effect on genome architecture, and its residence time on DNA. Our molecular simulations show that the dissociation speed of a structural protein from a DNA polymer depends on the protein concentration, but 3d chromosomal structure also affects the dissociation kinetics.

INTRODUCTION

Bacterial transcription factors (TFs) are DNA-binding proteins that can dynamically regulate the involvement of RNA polymerase (RNAP) in transcription by reversibly binding to DNA (1,2). Conventionally, the binding of a TF to its DNA target site is considered sufficient for the functionality of the corresponding TF (i.e., activation or repression of the target gene). However, a growing body of work has demonstrated that the time that a TF spends along the genome (i.e., DNA residence time) could contribute to the regulation of TF functions (3–5).

There are various biomolecular mechanisms by which the residence time of a single TF can influence the transcription output (i.e., mRNA expression). For an activator type of TF, such as Rap1, a long residence time on the binding site can increase the probability of recruiting RNAP or other cofactors to initiate transcription (4). In this way, a gene can maintain its on state and increase the frequency or duration of mRNA expression, depending on the organism (6,7). For repressor TFs, a longer stay on the target site can sterically hinder the binding of an activator TF to the gene, thus

Submitted August 5, 2021, and accepted for publication March 1, 2022.
*Correspondence: aykut.erbas@unam.bilkent.edu.tr
Editor: Andrew J Spakowitz.
https://doi.org/10.1016/j.bpj.2022.03.002

preventing RNAP recruitment in the first place. Consequently, a longer residence time would extend the duration of such a repression mechanism (3). Some repressor TFs can directly block the way of a transcribing RNAP and stall transcription proportional to their DNA residence times (5). Repression can also be imposed by a rapid turnover rate of an activator TF on its binding site (i.e., short residence time) such that RNAP or other cofactors cannot bind stably even though the binding site is on average occupied by a TF (4). Overall, DNA residence time of a single TF could contribute to the gene expression by modifying the binding stability of transcription components.

Recently, a concentration-dependent mechanism referred to as facilitated dissociation (FD) has been discovered to alter the residence times of key bacterial TFs along with a wide array of DNA-binding proteins (8–19). The molecular mechanism of FD is explained by the competition between DNA-bound proteins and solution-phase binding competitors for the same binding site (20,21). The competition can be either for sites on the protein (if the competitor is DNA) or sites on the DNA (if the competitor is protein) (22). At low concentrations (i.e., the probability of encountering two proteins on the same binding site is low), a DNA-bound TF can dissociate spontaneously because of thermal fluctuations. At higher concentrations, a solution-phase protein can bind to the TF-DNA complex and shorten the residence time of the bound TF onDNA as compared with the spontaneous dissociation (SD). The solution proteins can either replace the original protein (rapid turnover) or form a highly unstable ternary complex, which can lead to an empty DNA binding site. In either case, FD leads to on average shorter DNA residence times of the bound TF on a single-binding-site level as the protein levels increase (12).

Remarkably, among the DNA-binding proteins exhibiting the FD type of dissociation in vitro are major nucleoid-associated proteins (NAPs), such as the factor for inversion stimulation (Fis) and HU with diverse transcriptional and structural roles (14,23). In single-molecule studies, DNA residence times of the proteins declined to minutes from hours in response to concentration increase on the order of several hundred nanomolars (8,12,13). At the cellular level, these NAPs can vary their concentrations even more drastically (24–26); Fis can increase its cellular concentration reversibly from vanishing levels to 60,000 copies/cell ($\sim$100 μM after assuming a cytoplasmic volume of 1 μM^3) in the exponential phase (25,27). Nonspecific NAPs, such as HU or H-NS, also undergo large concentration fluctuations at different stages of the bacterial growth cycle, but their levels do not drop below $\sim$ 10 μM ranges (24,28). In principle, such concentration fluctuations should easily result in an FD-like mechanism. Nevertheless, these and similar structural NAPs can also alter the 3d organization of chromosome by forming dense multiprotein-DNA complexes in a concentration-dependent manner (29–32). Consequently, elevated protein levels can change the very environment (e.g., 3d chromosome organization) from which the proteins dissociate and put the functionality of FD at the cellular level into question.

Consistently, when Fis molecules dissociated from either sparsely surface-grafted DNA binding sites or extended DNA chains or chromosomes, they exhibited faster off rates with increasing protein concentration (8,12,13). However, when Fis molecules took part in the coating and looping of DNA molecules, they were shown to form highly stable DNA-protein complexes (i.e., the DNA residence time is higher than the experimental time window) (30). In separate experiments, when competing Fis molecules were replaced by nucleic acid segments, residence times were also shown to decrease via a DNA-segmental type of FD (22), suggesting a potential relationship between chromosome organization and dissociation kinetics. Apart from specifically interacting Fis, nonspecifically interacting HU also exhibited a concentration-dependent DNA binding stability, which was shown to be highly sensitive to DNA substrate conformation and competitor DNA fragments in solution (31). Another nonspecific NAP, H-NS, exhibited a similar dissociation mechanism strongly dependent on the type of protein-DNA complexation that it forms (33). In accord, several pioneering particle-tracking studies on metalloregulator TFs, CueR and ZuR, provided evidence that DNA residence times can change with chromosome organization in live cells. However, the cellular abundance of those TF proteins is only on the order of $\sim$1 μM (34,35); thus, they cannot alter the chromosome structure, unlike the structural NAPs, such as Fis or HU. Altogether, the experimental evidence suggests that organizational changes in chromosomal structure resulting from DNA-protein complexation can affect the dissociation kinetics of the proteins. However, how the concentration variations of the proteins contribute to this effect is not clear and demands a systematic study. Such resolving would require focusing on specific and nonspecific proteins individually, at least in a native-like environment, which may be achieved via well-designed computational models.

Previous computational studies on FD replicated the experimentally observed concentration-dependent dissociation, albeit at elevated concentrations (12,20,36,37). The studies confirmed that FD can occur for a wide range of binding affinities, but the effect of increasing concentration weakens as the protein binding energy decreases. Notably, those studies focused mainly either on a single locus (modeled as a stretched and physically constrained DNA segment) (20,36) or sparsely end-grafted short (e.g., 20-basepair [bp]) DNA binding sites to accurately model the experimental setups (12,37). Therefore, whether FD can occur in the confinement of the bacterial volume when binding sites are located along a high-molecular-weight DNA polymer, whose conformation is coupled to NAP concentration, cannot be answered by those studies. Indeed, Fis and HU already exhibited chromosome condensation activities

via the formation of stable multiprotein complexes with DNA (29–31,38). Those multiprotein-DNA complexes, in turn, can significantly change the proteins' binding stability, suggesting that elevated concentration levels in vivo could lead to two opposing or reinforcing effects on the unbinding kinetics of DNA-bound NAPs.

In this study, we aim to demonstrate a latent regulation mechanism involving cellular NAP levels and higher-order chromosome organization by addressing the functionality of FD at the cellular level. Specifically, we focus on the interplay between NAP concentration, protein off rates, and protein-induced chromosome organization in a model cellular confinement by using a large-scale and coarse-grained molecular dynamics (MD) model of an *Escherichia coli* bacterium (Fig. 1). Similar coarse-grained polymer models have been used previously to study entropic and sequence-dependent contributions to the bacterial chromosome organization (39–41). Several other studies considered explicit effects of multivalent NAPs on chromosome organization by incorporating coarse-grained protein models. Those simulation studies show that nonspecific interactions can form protein-rich complexes with DNA (42). The dimeric nature of proteins (i.e., their ability to bind two DNA segments simultaneously) was shown to be important to replicate experimentally observed protein-DNA complexes, such as those elongated clusters formed by H-NS proteins (43). Yet, those studies did not consider protein dissociation kinetics and rather focused on structures formed by DNA and proteins.

In our simulations, to investigate protein dissociation and related FD effects, more than 100 specific (e.g., Fis) or nonspecific (e.g., HU) NAPs with dimeric nature are allowed to fall off simultaneously from their binding sites in the presence of up to several thousand copies of solution-phase proteins. The proteins can dynamically interact (i.e., unbind and rebind) with a high-molecular-weight self-avoiding DNA polymer and change the conformation of the polymer dynamically. This MD setup allows us to precisely track all the proteins in the 3d cell environment simultaneously without any need for molecular labels while monitoring their cumulative effect on the higher-order chromosomal structure. Thus, although our computational experiments suffer from common weaknesses of molecular simulations, such as reduced degrees of freedom (i.e., less molecular details) and shorter timescales as compared with the experiments, they can avoid typical limitations of in vivo single-cell experiments, such as proteins escaping from the 2d measurement volume or short bleaching times of fluorescence labels.

Interrogation of various protein concentrations and DNA-protein attraction affinities reveal that FD could occur in the cellular confinement, particularly when the chromosome has an open structure. At several tens of micromolar concentrations, the chromosome is collapsed by well-ordered

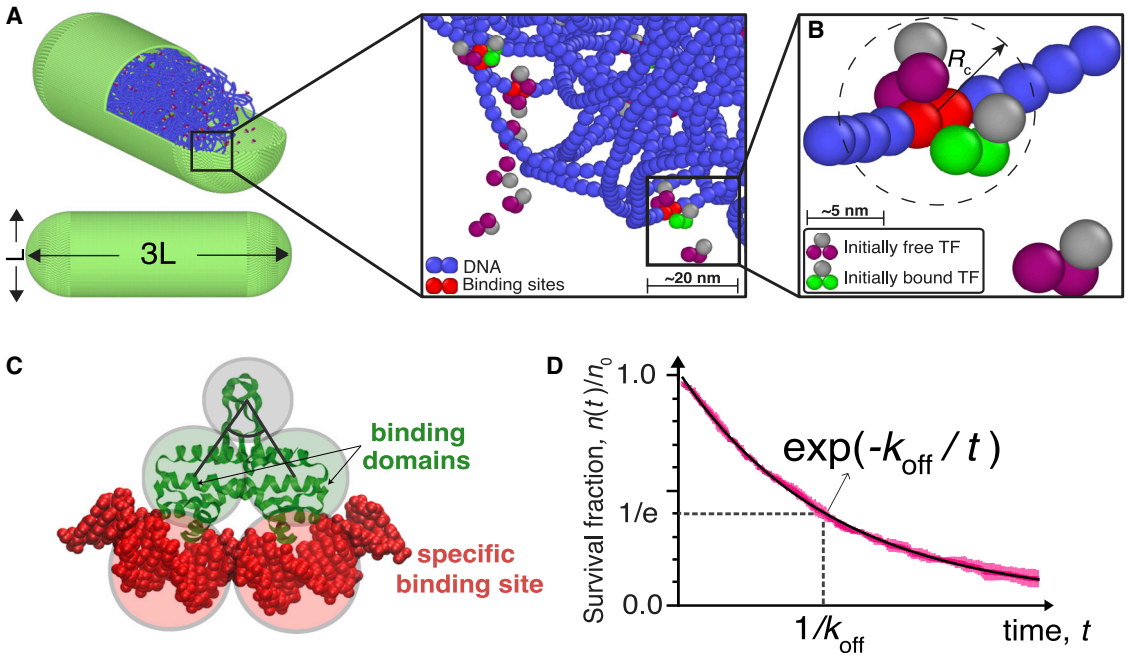

FIGURE 1 The schematics of the molecular dynamics simulation model. (*A*) The DNA polymer is confined inside a rigid concentric shell (light green beads) together with initially (i.e., at $t = 0$) bound and free proteins. The scale L corresponds to 200 nm. (*B*) Closer look into a single specific binding site (red beads) surrounded by nonspecific DNA (blue beads), with which bound and free dimeric proteins can dynamically interact. R_c is the cutoff distance centered around the binding site defined to determine the microscopically dissociated proteins. (*C*) Schematics of the coarse-grained protein model based on the dimeric Fis protein, where two binding domains (green beads) are joined by a hinge bead (gray). (*D*) Extraction of the off rate, k_{off}, from the time-dependent decay of the normalized number fraction of DNA-bound proteins (i.e., survival fraction), $n(t)/n_0$ (see Eq. 1). To see this figure in color, go online.

protein-DNA complexes consistent with previous studies (e.g., doughnut-shaped protein clusters, filamentous structures, and protein networks). Consequently, NAPs exhibit a rich behavior of dissociation kinetics depending on the sequence specificity of the proteins and chromosome organization.

MATERIALS AND METHODS

Molecular model of bacterial nucleoid

In MD simulations, we modeled bacterial DNA as a single circular polymer by using the coarse-grained "Kremer-Grest" (KG) self-avoiding bead-spring chain in implicit solvent (Fig. 1) (44,45). All steric and bond potentials are defined in the model (see Supporting material for details). The KG model provides a bead size of $b \approx 1\sigma$, where σ is the unit length scale of the simulations. The beads composing the DNA, proteins, and confinement have equal size. The single-bead size is mapped to real units by considering the crystal structure of the DNA-Fis complex (Fig. 1 *B* and *C*) (46); Fis has a binding site of ~20 bp, which is modeled by two beads in our model. This allows us to map the bead size to $b \sim 10$ bp in real units (i.e., the size of 10 bp is $b \sim 3.4$ nm after using 0.34 nm/bp). The DNA chain is modeled by $N = 12{,}000$ KG beads, which corresponds to 1.2×10^5 bp. Simulations with shorter chains do not affect our results qualitatively (see Fig. S1).

The proteins are based on the structure of DNA-bound Fis protein (Fig. 1 *B* and *C*). Although multivalency of the protein can be captured by two-bead models (12), we hypothesize that a three-bead model can recapitulate the steric interactions between proteins, as well as proteins and DNA, more realistically (Fig. 1 *C*). In the three-bead model, two DNA-binding domains are joined by a hinge, which provides a harmonic angle potential to penalize the deviations from the average "cherry" shape of the dimeric protein. After benchmarking various energy strengths for the angle potential, we use a strength of 12 kBT, which provides a stiffness similar to that of DNA polymer (see Fig. S2). The hinge does not bear any attraction toward DNA or other proteins. The semiflexible DNA (persistence length of ~ 150 bp or ~ 50 nm) and proteins are confined by a rigid concentric cylinder (also composed of beads) with an aspect ratio of 3 (Fig. 1 *A*). The volume of the confinement (1.7×10^{-2} μm^3) is adjusted in accordance with the volume fraction of the nucleic acids in *E. coli* (i.e., ~ 1%). The initial pervaded volume of DNA polymer is set to occupy ~ 40% of the cell volume to mimic the nucleoid structure (47).

In simulations, each model cellular confinement contains initially DNA-bound and initially unbound proteins (Fig. 1 *B*). These proteins are chemically identical unless otherwise noted. Although nonspecific proteins can bind to the entire DNA, specific proteins are allowed to bind a smaller number of dedicated binding sites composed of two beads (i.e., ~ 20 bp) unless otherwise noted. To determine the total number of binding sites, we consider ~3300 consensus sequences of Fis TF (48), which leads to an average inter-binding site distance on the order of 1000 bp. Hence we use $n_0 = 120$ binding sites for our $N = 12{,}000$ chains to obtain 1000-bp distance between binding sites. This value of n_0 is also high enough to perform statistical analyses for unbinding kinetics (37).

To monitor the concentration-dependent dissociation of DNA-bound proteins, we randomly added a prescribed concentration of excess competitor proteins in the model cellular confinement in addition to the n_0 initially DNA-bound proteins. Note that given the low volume fraction of DNA, only 1% of these proteins can be already DNA bound at $t = 0$. The total protein concentration in cells range between ~10 μM (only initially DNA-bound proteins) and ~210 μM, which correspond to 120 and 2225 protein copies per cell, respectively. Our maximum unbound protein concentration corresponds to 1 protein per ~60 bp, which is consistent with 60,000 Fis copies per cell, while intermediate concentration levels are consistent with the cellular abundance of NAPs, such as HU and H-NS (49).

A DNA-binding protein binds to DNA substrate via weak molecular interactions. Typically, the attraction between DNA and a small TF protein, such as Fis, is estimated to be around 20–30 kBT (i.e., 13–20 kcal/mol) (30,50,51), which can lead to hours-long dissociation times for an isolated protein-DNA complex (8,12). To observe the dissociation of the DNA-bound proteins within the practically achievable simulation times, we used specific DNA-protein binding strengths of $u_{SP} = 9$–12 kBT in our Lennard-Jones potentials. Each binding domain bead of the dimeric protein interacts with a specific DNA site bead via $u_{SP}/2$. We tested that the energy re-scaling only reduces dissociation times without changing the underlying physical mechanisms in accord with the universal behavior of FD (36) (see Figs. S3 and S4). To distinguish between specific and nonspecific binding, we also set a difference between nonspecific and specific protein-DNA attractions. Based on the 1000-fold difference in macroscopic dissociation constants of Fis for specific and nonspecific DNA binding (24,52), the minimum attraction strength of nonspecific DNA is set to $u_{NS} = u_{SP} - 7$ kBT. For instance, for $u_{SP} = 9$ kBT, the minimum default nonspecific attraction strength is $u_{NS} = 2$ kBT unless otherwise noted.

All simulations were run on LAMMPS MD package (53) on parallel 40-core processors. Error bars are calculated by averaging the results of a minimum of three independent runs and are not shown if they are smaller than the corresponding symbol size. Python NumPy package (54) and VMD or OVITO (55,56) are used for data analysis and the visualizations, respectively.

Calculation of off rates

At the beginning of a simulation (i.e., $t = 0$), initially DNA-bound proteins are initialized in direct contact with their binding sites. That is, the distance between a protein's binding domain bead and the closest binding-site bead is $R_0 \leq 1.0\sigma \approx 3.4$ nm. As time progresses in the simulations, the n_0 initially DNA-bound proteins leave their binding sites. The number of proteins remaining on their binding sites, $n(t)$, is monitored as a function of the simulation time, t. If a bound protein diffuses out of a spherical region defined by a cutoff radius, R_c, centered around the center of mass of the binding site (red beads in Fig. 1), the protein is tagged as dissociated. Note that after benchmarking various cutoff values of $R_0 < R_c \leq 4\sigma$, a minimal number of rebinding events is observed for $R_c = R_0 + 1\sigma \approx 2.0\sigma \approx 7$ nm and used as a criterion for dissociated proteins (see Figs. S5 and S6). Therefore, we probe the microdissociation of proteins to a distance roughly equivalent to the protein size (i.e., self-diffusion distance). If a dissociated protein rebinds to DNA, it is not counted in the surviving bound proteins, $n(t)$. The survival-fraction data are fit by a single exponential to determine the off rates,

$$n(t) \,/\, n_0 \;=\; \exp\left(-k_{\,\mathrm{off}} t\right), \tag{1}$$

where $k_{\,\mathrm{off}}$ is the off rate with the units of simulation time, which is matched to the self-diffusion time of a protein with a size of 6.8 nm (~250 ns) (43). A sample decay curve is shown in Fig. 1 *D*. Further details on the MD simulations and estimations are provided in the Supporting material.

RESULTS

The dissociation of specific DNA-binding proteins shows the characteristics of FD

To investigate the FD of specific proteins in the confinement of a prokaryotic cell, we monitor the initial dissociation of DNA-bound proteins off their specific binding sites in the absence or presence of prescribed concentrations of initially unbound proteins (Fig. 2). Once the proteins dissociate, they can rebind to DNA polymer at the same or another specific

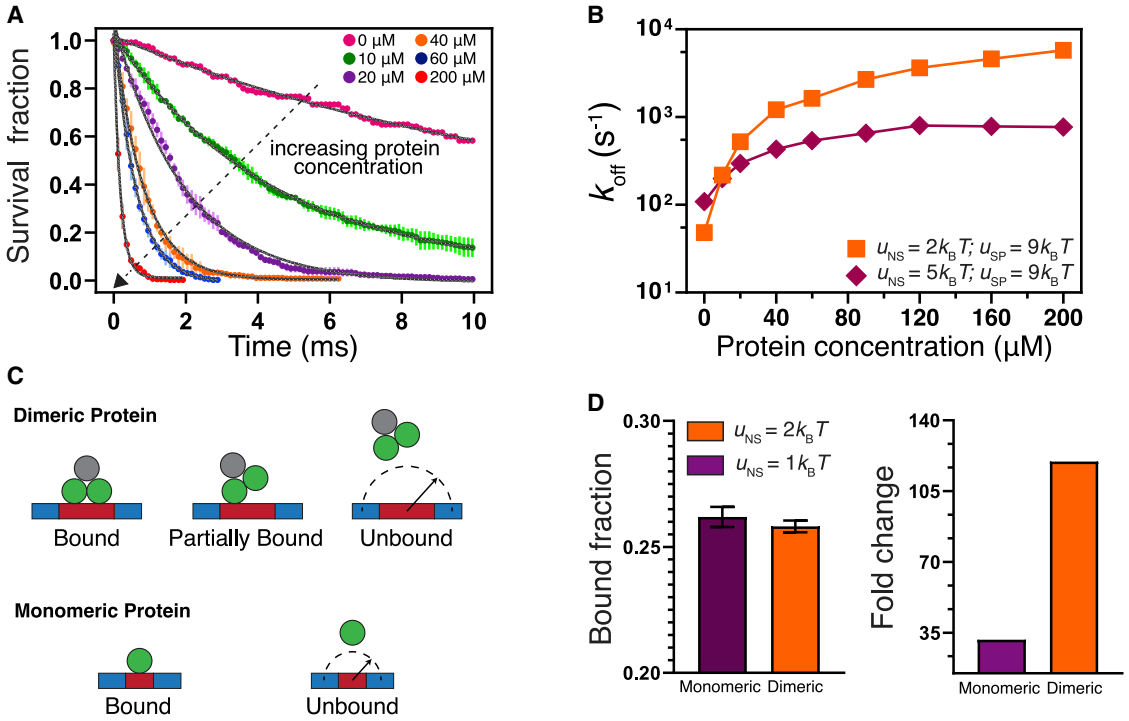

FIGURE 2 The evidence for the facilitated dissociation in the cellular confinement. (*A*) Representative rescaled survival fraction data of $n_0 = 120$ initially DNA-bound proteins for various concentrations of initially unbound proteins. The proteins interact with DNA via specific and nonspecific attractions of $u_{SP} =$ 9 kBT and $u_{NS} = 2$ kBT, respectively. The solid curves are the exponential fits (Eq. 1). The regions with lighter colors indicate the error bars. (*B*) The off rates extracted from the survival fraction data as a function of unbound protein concentration for various protein-DNA attractions. The data points are joined to guide the eye. (*C*) Monomeric and dimeric TF models at their bound and unbound states. The dashed half circles illustrate the cutoff distance used to determine whether a protein is bound or unbound. (*D*) Quasi-equilibrium bound fractions and fold changes in off rates of proteins on the specific binding sites obtained from the separate simulations with monomeric and dimeric protein models. The bound fractions are in the presence of initially 200 μM unbound protein levels with corresponding valency. Fold changes are calculated with respect to corresponding SD cases (i.e., no initially unbound proteins). To see this figure in color, go online.

site. Alternatively, the protein can bind to nonspecific DNA with a lower affinity or stay DNA-free inside the cellular volume (23).

One key parameter in our simulations is the protein-DNA attraction strengths that can provide realistic residence times for our model NAPs. Typical specific energy strengths of Fis range between $u_{sp} = 20$ and 30 kBT as estimated via theoretical calculations (51), experiments of Fis-assisted loop formation (30), and potential mean force simulations (50). Such interaction strengths can lead to residence times on orders of seconds to minutes (57), which are beyond the practical limits of current computational studies. Thus, in our simulations, we chose specific binding energies ranging between $u_{sp} = 9$ and 12 kBT, which are high enough to provide stable protein-DNA complexes but low enough to observe SD within the duration of our simulations (see Figs. S3 and S4).

In Fig. 2, we show representative dissociation curves of initially DNA-bound proteins leaving their specific binding sites to be replaced by solution-phase proteins at various concentrations. In the case of SD, for which bound proteins fall off from their specific binding sites in the absence of solution-phase proteins, the dissociation of DNA-bound proteins is significantly slow (i.e., less than 100% of the proteins leave their binding sites within the maximum simulation time) (top curve in Fig. 2 *A*). However, as the concentration of initially unbound proteins is increased, the dissociation curves decay more rapidly, indicating that DNA-bound proteins stay on average for a shorter time on their specific binding sites (Fig. 2 *A*). For instance, at a protein concentration of 60 μM (1 protein copy per 160 bp), almost all initially DNA-bound proteins leave their specific binding sites after several milliseconds (blue curve in Fig. 2 *A*). This concentration-dependent behavior of dissociation curves is robust and observed for higher DNA-protein attractions (Figs. 2 *B* and S3) and consistent with the previous dissociation measurements in the single-molecule experiments (8,12).

Next, to observe whether the dissociation responses follow a typical FD pattern, we extract the off rates by fitting each dissociation curve by a single exponential function (i.e., Eq. 1). As the binding attraction is increased or the concentration is decreased, the extraction of the off rates is rather limited because of the slow dissociation of

DNA-bound proteins (Figs. 2 *A* and S3). Hence in our off-rate calculations, we use a dissociation curve only if more than 40% of DNA-bound proteins dissociate in the corresponding simulation. As expected from the conventional FD behavior (8,12), the calculated off rates of the specifically binding proteins exhibit a consistent increase with the increasing concentration of initially free proteins (Fig. 2 *B*). Over a concentration range of 10–200 μM, the off rates accelerate up to 10-fold as compared with their SD values.

The overall profile of the off rates in Fig. 2 *B* is also consistent with the theoretical model (12,20): as the concentration increases, a linear increase in the off rates at the low concentrations (taking place within a concentration range of ~10–50 μM) is followed by a much weaker increase (Fig. 2 *B*). Notably, as the nonspecific attraction between the proteins and DNA becomes weaker (i.e., the value of μ_{NS} is dropped from 5 to 2 kBT), the effect of the concentration increase on the off rates becomes stronger (squares versus diamonds in Fig. 2 *B*). We will further discuss the effect of nonspecific interactions on dissociation kinetics in the following subsections. While the observed concentration dependence of the off rates qualitatively agrees well with the FD mechanism (8,12,23), the off-rate values in the simulations are higher than those observed experimentally, which we attribute to the re-scaling of the protein-DNA attraction energies. Nevertheless, the systematic increases in the off rates within the studied concentration range demonstrate the drastic effect of solution-phase proteins on the dissociation kinetics of specifically DNA-binding proteins in bacterial nucleoid.

Monomeric proteins have a weaker dissociation response than dimeric proteins

To ensure that the concentration-dependent effects we observe above are indeed FD, we decide to test the relation of FD to the multivalency of the DNA-binding proteins (20). Protein multivalency can allow a DNA-bound protein to visit intermediate binding states on DNA (e.g., a protein may bind to DNA via some, but not all, of its noncovalent inter-molecular interactions) (Fig. 2 *C*). In this way, the DNA-bound protein can partially expose the binding site for unbound proteins. Because the binding of a free protein to the exposed binding site becomes more likely with increasing (unbound) protein concentration, a state in which more than one protein shares a single binding site can occur. Consequently, this relatively less stable complex can accelerate the dissociation of the originally bound protein (8).

In our default dimeric protein model, the multivalency is achieved by the two independent binding domains (Fig. 1 *C*). We hypothesize that replacing all of our dimeric proteins with their monomeric counterparts should weaken or diminish concentration-dependent off rates in the simulations. This is mainly because a monomeric protein is composed of a single bead and thus can be either in a DNA-bound or free state and should exhibit no binding intermediates (Fig. 2 *C*).

While running our monomeric protein (i.e., single-bead) simulations, we choose to set the interaction strengths per bead to match those of a dimeric protein with specific $u_{SP} = 9$ kBT and nonspecific $u_{NS} = 2$ kBT attraction strengths. As we will discuss later, these interaction parameters do not lead to a compact chromosome structure for dimeric proteins and allow us to focus solely on protein-concentration effects. Nevertheless, monomeric proteins with $u_{NS} = 2$ kBT lead to a highly compact chromosome (see Fig. S7). Thus, we decide to adjust the nonspecific attraction of monomeric proteins to obtain identical quasi-equilibrium bound fractions for both dimeric and monomeric proteins (Fig. 2 *D*). Then, we use this setup to monitor the effect of solution-phase proteins in the calculated off rates with respect to the corresponding SD cases (i.e., when initially unbound protein level is zero).

In Fig. 2 *D*, we compare the fold change between the SD and 200 μM protein concentration in the off rates of monomeric and dimeric proteins unbinding from monomeric and dimeric binding sites, respectively. Note that total attraction strength is provided equally by two beads of the dimeric protein model, whereas in monomeric proteins, a single bead provides all attraction strength. Our simulations show that despite their similar quasi-equilibrium bound fraction levels, in the presence of 200 μM unbound proteins with corresponding valency, the off rate of dimeric proteins increases roughly 100-fold while the off rate of monomeric proteins at the same protein level increases only 26-fold (Fig. 2 *D*). This suggests that the effect of concentration on protein dissociation is correlated with the multivalency of the proteins.

The kinetic phenomenon that we observe here can be rationalized by considering a theoretical model proposing a step-by-step unbinding of a DNA-bound multivalent protein (8,20). Accordingly, in the absence of solution-phase proteins (i.e., SD), both dimeric and monomeric proteins must overcome an unbinding energy barrier, which leads to $k_{off}^{(0)} = 1/\tau_0 \exp(u_{SP}/k_BT)$, where $1/\tau_0$ is the off rate in the absence of any barrier. However, the dimeric protein is assumed to leave the DNA by unbinding one of its monomers first and then the other one, unlike the monomeric protein that unbinds all at once (Fig. 2 *C*). When there are unbound dimeric proteins in the solution with concentration c, they can bind to the binding site partially exposed by the dimeric protein. Consequently, off rate becomes dependent on the solution-phase protein concentration c as follows (8):

$$k_{off} = k_{off}^{(0)} + ck_1, \tag{2}$$

where ck_1 is the association rate constant of a monomeric unit of the dimeric protein in the units of inverse time. Thus, in our simulations, when there are no initially unbound proteins (i.e., $k_1 c \to 0$), both monomeric and dimeric

proteins are of similar off rates. As the free proteins are added to the cellular confinement, the second term in the above equation kicks in for dimeric proteins and accelerates the unbinding rate. Overall, based on our simulations with two different protein models, we conclude that the concentration-dependent phenomenon that we observe here for our specifically binding dimeric proteins is indeed FD.

Nonspecific attraction between DNA polymer and proteins affects the FD

The specifically interacting NAPs such as Fis can exhibit finite and measurable dissociation constants toward a large set of nonspecific sequences with diverse binding affinities (58). Further, NAPs such as HU or H-NS bind to DNA sequence nonspecifically, and in principle, their binding sites are surrounded by binding sites with equal affinity (24). Hence to systematically investigate the role of DNA-protein nonspecific interactions on the FD mechanism, we run simulations for various nonspecific attractions ranging as $0 \leq u_{NS} \leq u_{SP}$ by fixing the strength of specific DNA-protein attraction, u_{SP}. In doing so, we can model specifically interacting NAPs (i.e., $u_{NS} < u_{SP}$), as well as proteins interacting with the DNA sequence independently (i.e., $u_{NS} = u_{SP}$).

Our simulations reveal the distinct dissociation responses of specific and nonspecific DNA-binding proteins to the increasing free protein levels. Fig. 3 *A* shows the off rates for two biologically relevant concentrations, 20 and 60 μM (i.e., one protein per roughly 400 and 160 bp, respectively), as a function of the nonspecific attraction strength, u_{NS}. If the proteins interact specifically with DNA, their off rates increase as a smooth saturation function with increasing protein levels and undergo an apparent FD (Figs. 2 *A* and 3). That is, the higher the protein level is, the quicker the DNA-bound protein dissociates. However, as the nonspecific attraction between DNA and proteins is increased, the off rate becomes visibly independent of the protein concentration at a nonspecific attraction value of around $u^*_{NS} \sim 2/3 u_{SP} \sim 6 k_B T$ (Fig. 3 *A*). We observe this behavior also for higher values of the specific attraction (Fig. S4), suggesting that this phenomenon is not a side effect of the lower binding energies that we use in the simulations.

As the proteins distinguish less between specific and nonspecific DNA (i.e., $u_{NS} \rightarrow u_{SP}$), the dependence of the off rate on the concentration is completely reversed (Fig. 3 *A*): unlike the conventional FD, in which off rates increase with increasing concentration, the off rates of nonspecific proteins become slower as the concentration increases. This inverse FD effect is more evident when the off rates are plotted as a function of the protein concentration (Fig. 3 *B*). As the unbound protein concentration goes up, the off rate of nonspecific proteins slows down and reaches a plateau, at which the dissociation becomes roughly 10 times slower than the SD case (circles in Fig. 3 *B*).

To decipher the mechanism of this inverse FD effect, we analyze our simulation trajectories to distinguish between 1d sliding-dominated dissociation (e.g., protein leaves the binding site by sliding along the DNA), 3d escape (i.e., protein becomes DNA free), and segmental jump (i.e., protein jumps from its binding site to another remote DNA segment) (Fig. 3 *C*). To achieve this, we monitor the positions of newly dissociated TFs. If a TF is found attached to any neighboring DNA bead with a range of five beads (or 50 bp) upstream or downstream its original binding site, the TF is considered to have undergone 1d sliding. If the TF is present near the rest of the beads of the DNA polymer, it is marked as the segmental

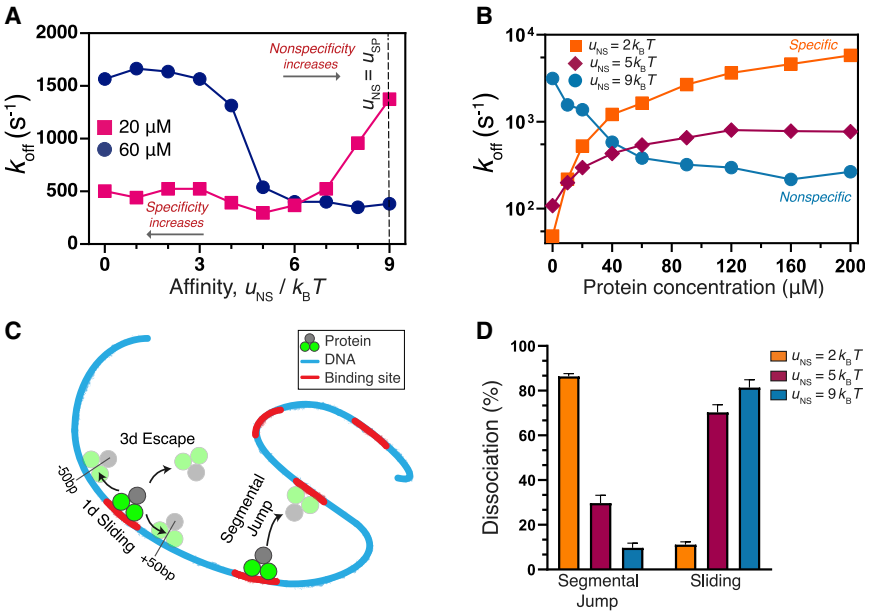

FIGURE 3 The role of nonspecificity on the facilitated dissociation of proteins. (*A*) Off rates as a function of nonspecific protein-DNA attraction for two initially unbound protein concentrations of 20 and 60 μM. The vertical line refers to nonspecifically interacting proteins. (*B*) The calculated off rates as a function of the initially unbound protein concentration. The proteins can bind to DNA via specific and nonspecific interactions (i.e., $u_{SP}>0$ and $u_{NS}>0$) or bind to DNA only specifically (i.e., $u_{SP}>0$ and $u_{NS} = 0$). The specific attraction is $u_{SP} = 9$ kBT in all cases. The data points are joined to guide the eye. (*C*) Schematics of 1d sliding, 3d escape, and segmental jump of the DNA-bound proteins. (*D*) The percentage of proteins undergoing the dissociation modes defined in (*C*) at 60 μM. To see this figure in color, go online.

jump. If the TF did not dissociate via any of the two mechanisms, it is labeled as a free protein. Our analysis shows that specific proteins dissociate mostly (i.e., >80%) via segmental jump, while nonspecific proteins leave their binding sites mostly by 1d sliding (Fig. 3 *D*). Notably, the 3d escape is negligible for our sampling intervals of TF positions. These dissociation patterns suggest that the decrease in off rates of nonspecific proteins with increasing concentration is a consequence of slower 1d sliding, possibly because of proteins coating the nonspecific DNA nearby the binding site at elevated concentrations. We will further discuss the effects of specific and nonspecific proteins on chromosome organization in the following sections.

Overall, our simulations suggest that nonspecifically and specifically interacting structural proteins can exhibit marginally different kinetic responses to the increasing concentration of solution-phase proteins. In the following sections, we discuss these findings further by considering the relationship between chromosomal structure and dissociation kinetics.

High NAP concentration leads to chromosome compaction

Nonspecific interactions between NAPs and DNA are known to contribute to chromosome organization (30,38). Thus, we suspect that as the proteins condense on the DNA polymer, the resulting structural alterations could affect the FD of the DNA-bound proteins by the solution-phase proteins. To quantify the chromosomal structural changes, we analyze the chromosome organization both visually and by calculating the quasi-equilibrium radius of gyration of the DNA polymer, R_g, for various nonspecific attraction strengths and protein concentrations.

In our simulations, the initial configuration of the nucleoid structure fills roughly 40% of the overall cellular volume (Fig. 1 *A*). Depending on the protein levels and protein-DNA nonspecific attraction, the nucleoid either swells to fill the entire cell volume or collapses down to its smallest size, which is dictated by the bead-bead steric interactions (Fig. 4 *A–D*). In a protein-free system, the size of the chromosome is mainly determined by the dimensions of the cellular confinement. For our chromosome model, this number is $R_g \sim 170$ nm (the horizontal line in Fig. 4 *A* and upper panels of Fig. 4 *B–D*). Notably, this open chromosome structure is in accord with the Hi-C contact maps of Fis-deficient cells (59,60).

We first consider the case where proteins can bind the whole DNA but cannot form stable complexes with nonspecific DNA because of the low protein-DNA nonspecific attraction (in our simulations, this attraction limit is $u_{NS} \leq 3k_BT$). In these cases, the chromosome size has no apparent dependence on the protein concentration, and R_g is close to its protein-free value (Fig. 4 *A* and *B*). However, even in this swollen chromosomal structure, the proteins form clusters by bridging multiple specific (high-affinity) binding sites (left panel of Fig. 4 *E*). Because, in our model, there are no protein-protein or DNA-DNA attractions, such DNA bridges are possible only if proteins are shared by multiple specific sites (43,61). Although the bridges anchor multiple protein-free DNA segments, they are unable to compact the chromosome even at the highest protein levels that we use here (i.e., 200 μM or 1 protein per 60 bp). Hence the resulting swollen polymer structure pervades the entire cellular volume regardless of the protein level (Fig. 4 *B*). Notably, the protein clusters are dynamic and contain on average several tens of proteins, and the average cluster size is not affected by the protein concentration (Fig. S8).

Contrarily, if proteins can form stable complexes with both specific and nonspecific DNA, chromosome compaction exhibits a highly concentration-dependent behavior (Fig. 4 *A–D*). At low protein levels (i.e., lower than 20 μM or 1 protein per less than ∼ 400 bp), we observe evenly distributed nodes composed of several tens of proteins for both specific and nonspecific proteins (Fig. 4 *C–E*). As the protein concentration is increased further (>20 μM), proteins form larger (i.e., >40–50 proteins) and inter-connected multiprotein-DNA complexes (Figs. 4 *C–E* and S8). For specific proteins, we observe in our simulations that genomic regions containing relatively high-affinity binding sites act as nucleation sites for the formation of larger clusters (Video S1). Nonspecific proteins, in contrast, tend to form more 1d-like structures as compared with the specific ones, as shown in Fig. 4 *E*, in accord with the previous observation with model H-NS proteins (43). As the protein concentration is increased gradually, the chromosomal structure shrinks in a concentration-dependent manner (Fig. 4 *A–D*). Notably, even though there is no torsional component in the DNA-polymer model, circular structures, in which multiple DNA segments are juxtaposed by specifically interacting proteins, emerge (Fig. 4 *E*).

At the highest protein level that we consider here (i.e., 1 protein per 60 bp), the chromosome completely collapses into a globular structure similar to a polymer chain in poor solvent conditions (bottom panels in Fig. 4 *C* and *D*). Such collapse requires a nonspecific attraction greater than $u_{NS} > 3$ kBT) (Fig. 4 *A*). Notably, nonspecific proteins seem to be more effective in compacting the chromosomal structure (Fig. 4 *A*). These protein-induced structures are consistent with the high-resolution force-spectroscopy images of Fis-induced compaction of isolated DNA segments at similar protein levels (38). Overall, our simulations show that nonspecific interactions significantly increase the capability of structural NAPs to compact the chromosomal structure in a concentration-dependent manner.

Chromosome compaction affects protein-dissociation kinetics

Returning to our discussion on dissociation kinetics, in our calculations, the average off rates are determined on the first

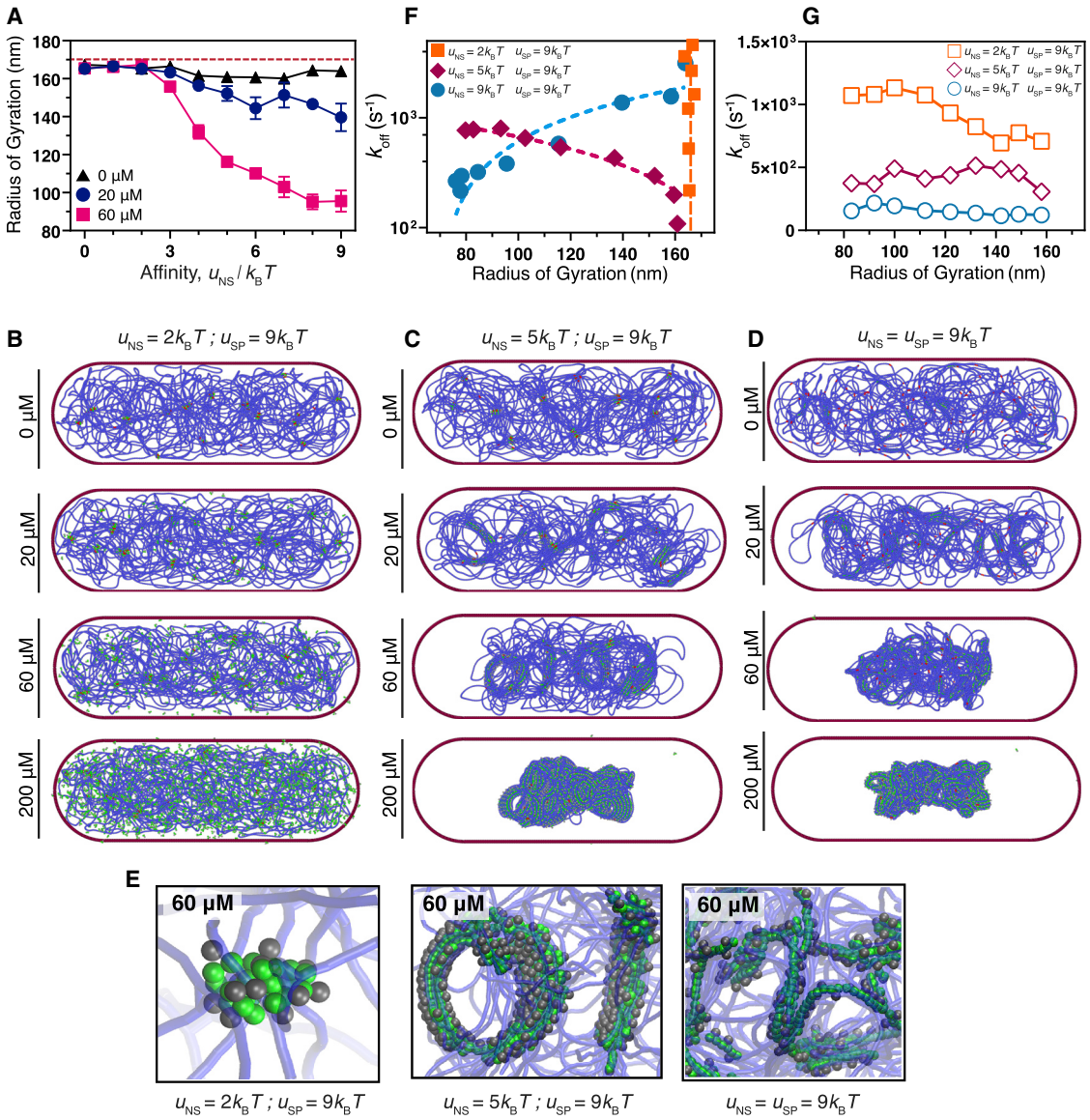

FIGURE 4 Chromosome compaction and facilitated dissociation. (*A*) The calculated values of radius of gyration, R_g, of chromosome structure as a function of nonspecific attraction for three concentrations of initially unbound proteins. The vertical line indicates the protein-free nucleoid size in the simulations. (*B–D*) Representative snapshots of chromosomal structures for the initially unbound Fis concentrations of 0, 20, 60, and 200 μM (left-to-right) for a specific (SP) binding energy of $u_{SP} = 9$ kBT. Initially bound and unbound proteins are both marked by the same colors in the snapshots. The beads of the cell boundary are indicated by magenta. (*E*) Close-up views of protein clusters for various concentrations for the cases in (B)–(D). (*F*) The off rates versus R_g for various protein-DNA cases. The dashed curves are linear regression fits to guide the eye. (G) Off rates were obtained in a restrained DNA-polymer system as a function of preset R_g values. To see this figure in color, go online.

dissociation events of the initially DNA-bound proteins. In some cases, the average timescales of chromosomal organization and protein dissociation are not well separated (i.e., a quasi-equilibrium polymer configuration is not reached at the instant of initial dissociation) (Fig. S9). However, a comparison between the off rates and chromosome size could serve to identify the mechanism of the different concentration responses of nonspecific and specific DNA-binding proteins because nonspecificity drastically affects the chromosomal compaction (Fig. 4 *A–E*).

In Fig. 4 *F*, we compile the off rates of various protein-DNA interaction scenarios from Figs. 2 and 3 and plot them as a function of the corresponding quasi-equilibrium chromosome size, R_g. Note that because the quasi-equilibrium chromosome size depends on the protein concentration, re-plotting the off rates as in Fig. 4 *F* could serve as an alternative way of probing the relationship between NAP concentration and dissociation kinetics by observing mesoscale chromosome size. The inverse concentration response of the off rates of specifically and nonspecifically

DNA-binding proteins shown in Fig. 3 *B* also persists in Fig. 4 *F*. For specific proteins, the fastest off rates correspond to the minimum size of the chromosomal structure (at the maximum protein level). Contrarily, for nonspecific proteins, the fastest off rates correspond to the most open chromosomal structure (at the minimum protein level) (Fig. 4 *F*). For completeness, we also add the data for the proteins that bind to nonspecific DNA very weakly while forming stable complexes with a limited number of specific DNA sites (orange symbols in Fig. 4 *F*). Because these proteins cannot change the genome size, R_g, by themselves in our simulations (Fig. 4 *B*), their off rates depend only on protein levels and accumulate at the maximum R_g value.

Our simulations suggest that if nonspecific attractions are strong enough, high NAP levels can decrease the chromosome size and consequently increase the nucleic acid concentration within the pervaded volume of the chromosome (Fig. 4 *A*). This compaction may cause a DNA-segmental type of FD (22) or change the frequency of protein rebinding events to the DNA polymer (62). Hence to decouple the compaction (or expansion) of the chromosome from the protein dissociation, we restrain the self-avoiding walk configuration of the DNA polymer at prescribed R_g values (i.e., no thermal fluctuations occur for the polymer) and run a large set of protein-dissociation simulations (Fig. 4 *G*). In these simulations, the proteins can unbind from and bind to the DNA but are unable to change its conformation.

If we choose an unbound protein level of 60 μ M, for which we observe a considerable amount of FD-related effects (Figs. 2 and 3), the effect of R_g variations on calculated off rates shows a systematic dependence on protein-DNA nonspecific interaction strength (Fig. 4 *G*). For specific proteins that interact weakly with nonspecific DNA (i.e., $u_{SP} \gg u_{NS}$), off rates are the highest regardless of the chromosome size (squares in Fig. 4 *G*). As the nonspecificity is increased, off rates slow down for the entire range of R_g cases (circles in Fig. 4 *G*).

Among the three protein types we consider here, off rates of the proteins that can bind to the whole DNA nonspecifically (i.e., $u_{SP} = u_{NS}$) visually have no dependence on R_g. Given that the main mechanism of dissociation for nonspecifically interacting proteins is 1d sliding along DNA (Fig. 3 *C* and *D*), and chromosome compaction in principle should not interfere with such 1d sliding, the weak dependence of off rates of nonspecific proteins on R_g is consistent with the data in Fig. 4 *G*. Contrarily, for proteins interacting weakly with nonspecific DNA, decreasing R_g increases the calculated off rates. For those proteins, the segmental jump is the main mode of dissociation (Fig. 3 *C* and *D*). Consistently, as R_g decreases, the average distance between DNA segments (i.e., polymer correlation length) decreases, which in turn can accelerate the off rates via segmental jumps by shortening average distances between DNA segments (Figs. 4 *G* and S10). Overall, our MD simulations suggest that chromosome compaction can affect the off rates of specific DNA-binding proteins, while compaction has a weak effect on the dissociation of nonspecifically interacting proteins because of different dissociation modes of two protein types.

DNA-bound proteins are replaced by both lower- and higher-affinity proteins via FD

So far in our simulations, the initially DNA-bound and unbound proteins have an equal binding attraction toward the DNA. Nevertheless, various NAPs and their mutants can coexist and compete for the same binding site with relatively small differences in their affinities (52,63). For instance, dissociation constants of K94A mutant and wild-type Fis differ by a factor of ~ 4 (52), which may result in $\sim$1 kBT difference in the DNA-protein attraction (see Supporting material for calculations). Moreover, DNA-bound Fis/HU was shown to exchange with HU/Fis molecules from solution in single-molecule experiments, indicating the heterotypic nature of FD (8). Similarly, H-NS proteins were shown to be displaced by *Salmonella enterica* regulator protein SsrB (33).

To reveal the competition between DNA-bound and free proteins from solution but with relatively lower/higher affinities, we perform additional simulations by setting an attraction difference of $\sim$1 kBT between the initially unbound and initially DNA-bound proteins. For simplicity, we choose $u_{SP} = 9$ kBT and $u_{NS} = 2$ kBT for initially DNA-bound proteins, for which the protein levels have no effect on the chromosome size (Fig. 4 *A* and *B*). Our simulations show that both relatively lower- ($u_{SP} = 8$ kBT) and higher-affinity ($u_{SP} = 10$ kBT) proteins are able to accelerate the dissociation of the DNA-bound proteins efficiently (Fig. 5 *A*). However, the solution-phase proteins are more effective in stripping the lower-affinity DNA-bound proteins off the DNA: solution proteins with $u_{SP} = 10$ kBT can facilitate

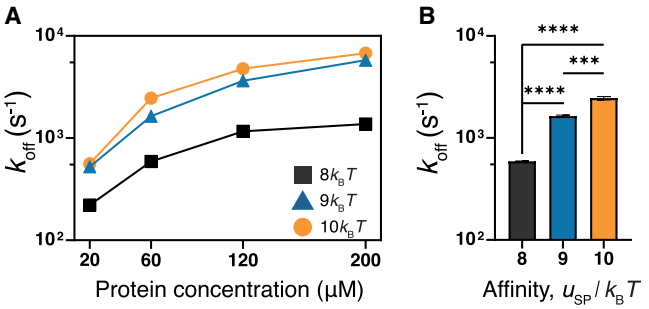

FIGURE 5 Heterotypic behavior of FD. (*A*) The off rates of proteins that interact with DNA with a specific binding strength of $u_{SP} = 9$ kBT for various concentration of initially unbound proteins. The specific DNA binding attraction of the initially unbound proteins is $u_{SP} = 8$, 9, or 10 kBT. In all cases, the nonspecific attraction is $u_{NS} = 2$ kBT. (*B*) The off rates at a concentration of 60 μM for three cases, when the initially unbound proteins have lower, equal, and higher affinity than initially DNA-bound proteins (unpaired, 2-tailed, Student's *t*-test). To see this figure in color, go online.

the off rate of $u_{SP} = 9$ kBT proteins approximately seven times more as compared with the initially free $u_{SP} = 8$ kBT proteins (Fig. 5 *B*). This suggests that even a small difference in affinities can play a key role in hierarchical dissociation of the proteins on a DNA.

DISCUSSION

To summarize, our extensive coarse-grained MD simulations, where the DNA-bound proteins are allowed to leave their binding sites along a self-avoiding, circular, and confined DNA polymer, show that both specific and nonspecific NAPs modulate their off rates depending on their cellular concentration levels. As the concentration of solution-phase (DNA-free) structural proteins increases, the protein off rate increases for specifically DNA-binding proteins but decreases for nonspecific proteins (Figs. 2 and 3). Detailed analyses of our simulation data reveal that specific proteins leave their binding sites by mostly jumping to a remote DNA segment. As nonspecific interactions between proteins and DNA increase, 1d sliding becomes the primary mechanism for dissociation (Fig. 3 *C* and *D*). For the same reason, nonspecific proteins are less prone to be influenced by chromosome compaction as compared with specially DNA-binding proteins (Fig. 4 *G*). Further, the simulations, where DNA-bound and solution-phase proteins have different affinities, demonstrate that the affinity determines the winner of the kinetic competition between the two different protein species competing for the same binding site, and the proteins with higher affinity can shorten the residence time of lower-affinity DNA-bound proteins (Fig. 5). Our simulations also show that nonspecific DNA-protein attraction has a substantial effect on the off rates of proteins dissociating from a folded chromosomal structure even though the proteins unbind from their specific binding sites (Fig. 2 *B*). In the following subsections, we will discuss in more detail our findings in the context of DNA residence times and gene regulation.

Concentration-dependent residence times of NAPs can have regulatory effects on transcription

As bacterial DNA-binding proteins, TFs demonstrate sequence-specific recognition and binding behaviors. They control the flow of the genetic information via promoting or repressing transcription by enhancing the recruitment of RNAP (or cofactors) or preventing its binding to target DNA. Hence mRNA expression can be initiated or halted. The first step to this process is the binding of a TF to its target site. When the cellular concentration of the TF increases, the probability of the protein to find its DNA target site increases linearly with the concentration (64). Once the TF binds to its recognition site, upregulation or downregulation of the corresponding gene occurs. However, this view implicitly assumes that (1) the concentration affects only on rates (i.e., association rate) but has no effect on the off rates, which is defined as the reciprocal of the residence time of the protein on its DNA target site; and (2) once the TF is bound to its target site, how long it stays there does not change its transcriptional output (e.g., mRNA expression by the cell).

A series of in vitro single-molecule studies have already challenged the first assumption and show that off rates of initially DNA-bound Gfp-Fis or HU become faster as the solution-phase concentration of the proteins is increased (8,12,13). Several computational studies mostly based on the single-molecule experimental setups (i.e., protein dissociation from constrained DNA segments or isolated and stretched chromosomes) also supported those observations (12,36,37). Our simulations go beyond those in vitro single-molecule experiments/simulations and demonstrate that structural dual-purpose proteins can exhibit concentration-dependent dissociation patterns also in a nucleoid-like environment, in which protein levels are directly coupled to chromosome organization. Our findings suggest that sequence-specific proteins such as Fis can stay shorter on their target sites with increasing Fis levels, and thus may couple their transcriptional activity with the duration of DNA occupancy. Proteins with no sequence specificity such as HU, in contrast, can maintain their binding positions longer as their cellular levels increase. This property can allow them to form stable higher-level protein complexes and limit the gene accessibility effectively while facilitating the disassembly of the complexes as the protein levels decline (Fig. 3). This view is also consistent with long DNA occupancy times of HU and H-NS proteins (i.e., 99% of the total target search time), which can assemble into large protein clusters on a DNA (65). In addition, a TF protein may respond differently to the concentration fluctuations depending on DNA sequences surrounding a promoter site. If the nonspecific and specific affinities of the protein are too close, the protein can exhibit a mixed response to the increased concentration of solution-phase proteins.

The second assumption to challenge is whether the transcription output of a gene depends on the residence time of the corresponding regulator. The competition chromatin immunoprecipitation experiments on the *Saccharomyces cerevisiae* Rap1 TF protein showed a direct correlation between the DNA residence time and transcriptional output: while transcriptional initiation, RNAP recruitment, and cellular transcript levels were all coupled to long residence times, low transcript levels were correlated with rapid unbinding even though DNA occupancy of the protein was similar in both cases (4). Another *Saccharomyces cerevisiae* TF, Abf1, has also exhibited one order of magnitude variation in the off rates on different binding sites, each of which is related to a different functionality (5). Interestingly, on the sites with relatively higher residence times, Abf1 seems to roadblock a transcribing RNAP more efficiently

as compared with the sites with lower residence times. More recently, by tuning DNA residence times via altering the number of nucleotide-recognizing repeat domains of transcription activator-like effectors (TALEs), residence-time-dependent repression of the glucocorticoid-receptor-activated gene SGK1 by TALE was studied (3). In those well-controlled systems, longer residence times were correlated with low transcript levels (i.e., stronger repression). In a separate study, the same group also studied the activation by TALE and showed that longer residence times on the target site can enhance transcription by allowing more efficient recruitment of transcription components (e.g., RNAP or cofactors) (6). Notably, although the aforementioned experiments did not address the concentration dependence of TALE dissociation, TALEs were shown to displace one another along the DNA (16). Interestingly, our analysis on the approach paths of competitor proteins shows that most competitors slide along the DNA to reach occupied binding sites (see Fig. S11). Thus, based on those findings and our results, we can postulate that if the residence time of a TF affects its transcription output, any physiological input modulating the residence times, such as the concentration of binding competitors, can also be a regulatory component. In the case of dual-purpose TFs (i.e., Fis), this modulation is intermingled with alterations in chromosome structure induced by the protein itself.

A tentative molecular picture for NAP-induced chromosome compaction

The high-resolution contact maps of *E. coli* chromosomes revealed a correlation between the high expression levels and chromosome structures that are rich in short-range contacts (60). Furthermore, several fluorescence studies demonstrated that Fis, along with HN-S and RNAP, can form foci in bacterial cells growing rapidly (66,67). The 3d STORM studies demonstrated that although Fis and HU can localize in large interconnected protein complexes (i.e., >200 nm), H-NS can oligomerize into discrete nodes anchoring distant loci (67). High-resolution MD models harvesting Hi-C data revealed a higher density of AT-rich sequences near the central section of bacterial volume (39), suggesting large assemblies of NAPs. Our simulations may present a molecular picture for the formation of such potentially transcriptionally active protein-DNA structures in a concentration-dependent manner.

At low protein concentrations (i.e., ∼10 μM), site-specific NAPs mainly manage to bridge multiple specific DNA binding sites into protein clusters (Fig. 4 *E*). These clusters are spread evenly throughout the relatively open bacterial chromosomes, consistent with super-resolution fluorescence microscopy of H-NS (67). Further, multiscale loop-like structures that are poor in high-affinity sites are anchored by these protein clusters (Fig. 4 *B*), confirming that such high-affinity sites can be functional in organizing DNA (61,68). Noteworthy, in our quasi-equilibrium configurations, the nonspecific DNA segments are mostly protein free except those neighboring the specific sites, suggesting the role of specific sites in the initiation of protein-DNA complexation from high-affinity sequences (61,69).

As the concentrations of structural NAPs approach their in vivo peak levels (i.e., ∼50 μM for Fis or ∼40 μM for HU), two distinct behaviors emerge depending on the binding mode of the protein. For specifically interacting Fis-like proteins, the protein clusters become fewer on merging, indicating the higher-order organization of specific DNA binding sites (Fig. 4 *C*; Video S1). For nonspecifically interacting proteins (e.g., HU), protein-DNA complexes tend to form elongated structures bridging multiple DNA segments (Fig. 4 *D* and *E*). We should underline that these protein-DNA assemblies emerge despite the absence of a net attraction between the proteins and induce an attraction between remote DNA segments as observed for H-NS (43). At excess protein levels greater than ∼100 μM, protein-DNA complexes shrink the chromosomes into highly compact structures (Fig. 4 *C–E*). All proteins are trapped inside or on the surface of the structures. Further, our simulations also suggest that nonspecifically interacting proteins seem to compact the chromosome more efficiently (Fig. 4 *A*) even though they tend to form filamentous protein-DNA complexes. Such compact DNA structures can act like steric filters and may exclude the large-size macromolecules (i.e., ribosome) from the nucleoid (67).

For proteins that interact with DNA mostly specifically (e.g., their diffusion coefficients in bulk and on nonspecific DNA are similar), our simulations suggest a strong conventional FD but no protein-induced compaction (Fig. 4 *B*). Interestingly, the lack of H-NS was shown to cause minimal changes in the nucleoid volume as well (47), suggesting that such nonspecific NAPs may undergo FD at least in a loose chromosomal structure. Nevertheless, the compaction of the chromosome by other structural NAPs can also change the DNA residence times of these proteins in a chromosome-organization-dependent way (34).

Chromosome organization can affect the facilitated dissociation response of DNA-bound proteins

The 3d chromosome structure is another component of transcriptional regulation (70–72). Chromosome compaction or loosening by structural NAPs can affect the recruitment of RNAP by changing the porosity of nucleoid (73). Our simulations suggest that alterations in the 3d chromosomal organization by NAPs can change the residence times of DNA-binding proteins (Fig. 4 *G*) and thus could be a modulator of gene regulation. Our MD simulations at prescribed chromosome-compaction levels suggest that this architectural regulation can vary for specific and nonspecific NAPs differently (Fig. 4 *G*). As nonspecific protein

concentration is increased, DNA segments are coated by elongated multiprotein complexes (Fig. 4 *E*). Because nonspecific proteins tend to leave their initial binding positions mostly by sliding toward neighboring binding sites (Fig. 3 *D*), the dissociation of an initially DNA-bound protein can be blocked by the proteins occupying neighboring binding sites. Hence, unlike specific proteins, nonspecific proteins exhibit a decaying off rate (longer residence times) with increasing solution-phase protein concentration. We should note that a TF's residence time does not necessarily have to be coupled to its ability to change chromosomal architecture. Even though the TF has no structural roles, alterations in chromosome organization can, for instance, promote segmental jumping between binding sites. Accordingly, the opposite responses of DNA residence times of apo and holo forms of metal-sensing TFs against chromosome compaction in live *E. coli* cells may be related to the phenomenon that we observe in our simulations (34,35).

FD, chromosome organization, and the functional diversity of Fis

Fis can participate in the regulation of more than 200 genes, including itself either as an activator or repressor necessary for growth, replication, and energy metabolism (25,52,74–76). Despite the high coarse-graining level of our dimeric protein model, our simulations could offer some clues about the broad functional diversity of Fis, as follows: (1) during the early stages of the growth, a gradual increase in Fis levels can modulate Fis residence times differently on different target sequences via FD; (2) as Fis concentration increases, its negative autoregulation capacity may decrease via FD (i.e., it cannot exclude RNAP effectively from the target sites because of fast turnover rates); particularly, this behavior can pursue through the lag phase to the early exponential phase; and (3) Fis could also lead to a temporal DNA compaction via protein-dense clusters at the regions containing Fis-regulated genes. Depending on the affinity of nonspecific sites surrounding the gene or the physical proximity of other specific sites nearby the gene, DNA compaction may inhibit RNAP's access to these gene-rich regions in a selective way.

To determine whether there is a correlation between Fis concentration and transcriptional activity, we revisit the time courses of cellular Fis and transcript levels under nutritional upshift from the literature (see fig. 2 of Ref. 25). Because the expression of Fis is significantly regulated at the transcriptional level, protein abundance is expected to be similar to the transcript levels with a time lag of ~10 min (25). Accordingly, when the cellular level of Fis reaches halfway through its maximum, the transcript level of Fis is already at its maximum. Consistently, the available DNA microarray expression profiles show a cumulative upregulation pattern for Fis-regulated genes within the early exponential phase (75). Once the Fis level attains its maximum at around >50 μM (i.e., the level at which we observe high DNA compaction and dense protein-DNA arrays in our simulations), Fis levels begin to decrease (25,75). The decrease continues from the early logarithmic phase to the stationary phase. Within this interval, the transcript levels of Fis also decrease from its peak level to vanishing values, suggesting a decreasing regulatory activity of Fis. We speculate that this reduction could be because of DNA compaction and/or dense protein clusters that can extend the residence times of Fis on DNA and thus its repressive activity.

As a final remark, the chromosome model we use here oversimplifies various physical and chemical properties of the genome while maintaining its major polymer properties. For instance, our model captures semi-flexibility of double-stranded DNA but cannot capture supercoiling of DNA by NAPs because of the absence of dihedral potentials (such approach would also require special coarse-grained protein models that can distort double-stranded DNA in protein-specific ways). We also assume a simplistic view of genome sequence by defining only two sets of binding interactions for specific and nonspecific binding sites. In reality, the protein-genome interaction landscape is more diverse, and the inclusion of this complexity is necessary, for instance, to accurately model genome-wide contacts in a model system (39). Notably, such diversity in attraction strengths could also lead to a power of law behavior for residence times (77). Yet, for the scope of this study, we think that our coarse-graining level of the genome is sufficient to obtain qualitative predictions on the concentration-dependent dissociation behavior of NAPs and protein-induced chromosome compaction.

In conclusion, our extensive MD simulations suggest that off rates of proteins falling off from a folded DNA polymer could be correlated with cellular protein levels and the chromosomal organizational changes that the proteins cause. Noteworthy, predictions suggested by our simulations should be considered with care given that the available timescale for the simulations is very limited (e.g., milliseconds), and many interaction cascades are integrated out. Nevertheless, the effects that we demonstrate here could contribute to regulatory roles of transcriptional protein by modulating their genome-wide residence times. An investigation of genome-wide off rates for proteins such as Fis by using dynamic chromatin immunoprecipitation or other experimental tools (4,5) would reveal such mechanisms. Finally, beyond prokaryotic cells, the phenomenon that we demonstrate here is very likely to be functional in eukaryotic cell nuclei as well, given that some structural DNA-binding proteins, such as histone, have already been shown to undergo FD (17,78).

SUPPORTING MATERIAL

Supporting material can be found online at https://doi.org/10.1016/j.bpj.2022.03.002.

ACKNOWLEDGMENTS

A.E. acknowledges J.F. Marko for the discussion on the Fis binding energies and Dr. B. Hekimoglu and Dr. E.J. Banigan for their careful reading of the manuscript. A.G.A. was supported by TÜBITAK 2247-CSTAR program. This research was supported by TÜBITAK 2232 (2018/4) 119C010.

REFERENCES

1. Browning, D. F., and S. J. W. Busby. 2004. The regulation of bacterial transcription initiation. *Nat. Rev. Microbiol.* 2:57–65.
2. Seshasayee, A. S. N., K. Sivaraman, and N. M. Luscombe. 2011. An Overview of Prokaryotic Transcription Factors. Springer Netherlands, Dordrecht, pp. 7–23.. https://doi.org/10.1007/978-90-481-9069-0_2.
3. Clauß, K., A. P. Popp, …, J. C. M. Gebhardt. 2017. DNA residence time is a regulatory factor of transcription repression. *Nucleic Acids Res.* 45:11121–11130.
4. Lickwar, C. R., F. Mueller, …, J. D. Lieb. 2012. Genome-wide protein-DNA binding dynamics suggest a molecular clutch for transcription factor function. *Nature.* 484:1–7.
5. de Jonge, W. J., M. Brok, …, F. C. Holstege. 2020. Genome-wide off-rates reveal how DNA binding dynamics shape transcription factor function. *Mol. Syst. Biol.* 16:1405–1416.
6. Popp, A. P., J. Hettich, and J. C. M. Gebhardt. 2021. Altering transcription factor binding reveals comprehensive transcriptional kinetics of a basic gene. *Nucleic Acids Res.* 49:6249–6266.
7. Stavreva, D. A., D. A. Garcia, …, G. L. Hager. 2019. Transcriptional bursting and co-bursting regulation by steroid hormone release pattern and transcription factor mobility. *Mol. Cell.* 75:1161–1177.e11.
8. Graham, J. S., R. C. Johnson, and J. F. Marko. 2011. Concentration-dependent exchange accelerates turnover of proteins bound to double-stranded DNA. *Nucleic Acids Res.* 39:2249–2259.
9. Loparo, J. J., A. W. Kulczyk, …, A. M. van Oijen. 2011. Simultaneous single-molecule measurements of phage T7 replisome composition and function reveal the mechanism of polymerase exchange. *Proc. Natl. Acad. Sci.* 108:3584–3589.
10. Joshi, C. P., D. Panda, …, P. Chen. 2012. Direct substitution and assisted dissociation pathways for turning off transcription by a MerR-family metalloregulator. *Proc. Natl. Acad. Sci.* 109:15121–15126.
11. Kunzelmann, S., C. Morris, …, M. R. Webb. 2010. Mechanism of interaction between single-stranded DNA binding protein and DNA. *Biochemistry.* 49:843–852.
12. Kamar, R. I., E. J. Banigan, …, J. F. Marko. 2017. Facilitated dissociation of transcription factors from single DNA binding sites. *Proc. Natl. Acad. Sci.* 114:E3251–E3257.
13. Hadizadeh, N., R. C. Johnson, and J. F. Marko. 2016. Facilitated dissociation of a nucleoid protein from the bacterial chromosome. *J. Bacteriol.* 198:1735–1742.
14. Chen, T.-Y., Y.-S. Cheng, …, P. Chen. 2018. Facilitated unbinding via multivalency-enabled ternary complexes: new paradigm for protein-DNA interactions. *Acc. Chem. Res.* 51:860–868.
15. Joseph, S. R., M. Palfy, …, N. L. Vastenhouw. 2017. Competition between histone and transcription factor binding regulates the onset of transcription in zebrafish embryos. *elifesciences.org.* 6:e23326.
16. Lebar, T., A. X. E. V. x0010D, …, R. Jerala. 2018. Polarized displacement by transcription activator-like effectors for regulatory circuits. *Nat. Chem. Biol.* 15:1–13.
17. Kilic, S., A. L. Bachmann, …, B. Fierz. 2015. Multivalency governs HP1. *Nat. Commun.* 6:1–11.
18. Luo, Y., J. A. North, …, M. G. Poirier. 2014. Nucleosomes accelerate transcription factor dissociation. *Nucleic Acids Res.* 42:3017–3027.
19. Gibb, B., L. F. Ye, …, E. C. Greene. 2014. Concentration-dependent exchange of replication protein a on single-stranded DNA revealed by single-molecule imaging. *PLoS One.* 9:e87922.
20. Sing, C. E., M. Olvera de la Cruz, and J. F. Marko. 2014. Multiple-binding-site mechanism explains concentration-dependent unbinding rates of DNA-binding proteins. *Nucleic Acids Res.* 42:3783–3791.
21. Åberg, C., K. E. Duderstadt, and A. M. van Oijen. 2016. Stability versus exchange: a paradox in DNA replication. *Nucleic Acids Res.* 44:4846–4854.
22. Giuntoli, R. D., N. B. Linzer, …, J. F. Marko. 2015. DNA-segment-facilitated dissociation of Fis and NHP6A from DNA detected via single-molecule mechanical response. *J. Mol. Biol.* 427:3123–3136.
23. Erbaş, A., M. O. de la Cruz, and J. F. Marko. 2019. Receptor-Ligand rebinding kinetics in confinement. *Biophysical J.* 116:1609–1624.
24. Ali Azam, T., A. Iwata, …, A. Ishihama. 1999. Growth phase-dependent variation in protein composition of the *Escherichia coli* nucleoid. *J. Bacteriol.* 181:6361–6370.
25. Ball, C. A., R. Osuna, …, R. C. Johnson. 1992. Dramatic changes in Fis levels upon nutrient upshift in *Escherichia coli*. *J. Bacteriol.* 174:8043–8056.
26. Dorman, C. J., and K. A. Kane. 2009. DNA bridging and antibridging: a role for bacterial nucleoid-associated proteins in regulating the expression of laterally acquired genes. *FEMS Microbiol. Rev.* 33:587–592. https://doi.org/10.1111/j.1574-6976.2008.00155.x.
27. Kelly, A., M. D. Goldberg, …, C. J. Dorman. 2004. A global role for Fis in the transcriptional control of metabolism and type III secretion in *Salmonella enterica* serovar Typhimurium. *Microbiology.* 150:2037–2053.
28. Verma, S. C., Z. Qian, and S. L. Adhya. 2019. Architecture of the *Escherichia coli* nucleoid. *PLoS Genet.* 15:e1008456.
29. van Noort, J., S. Verbrugge, …, R. T. Dame. 2004. Dual architectural roles of HU: formation of flexible hinges and rigid filaments. *Proc. Natl. Acad. Sci. United States America.* 101:6969–6974.
30. Skoko, D., D. Yoo, …, R. C. Johnson. 2006. Mechanism of chromosome compaction and looping by the *Escherichia coli* nucleoid protein Fis. *J. Mol. Biol.* 364:777–798.
31. Skoko, D., B. Wong, …, J. F. Marko. 2004. Micromechanical analysis of the binding of DNA-bending proteins HMGB1, NHP6A, and HU reveals their ability to form highly stable DNA−Protein complexes. *Biochemistry.* 43:13867–13874.
32. Remesh, S. G., S. C. Verma, …, M. Hammel. 2020. Nucleoid remodeling during environmental adaptation is regulated by HU-dependent DNA bundling. *Nat. Commun.* 11:1–12.
33. Walthers, D., Y. Li, …, L. J. Kenney. 2011. *Salmonella enterica* response regulator SsrB relieves H-NS silencing by displacing H-NS bound in polymerization mode and directly activates transcription. *J. Biol. Chem.* 286:1895–1902.
34. Chen, T.-Y., A. G. Santiago, …, P. Chen. 2015. Concentration- and chromosome-organization-dependent regulator unbinding from DNA for transcription regulation in living cells. *Nat. Commun.* 6:7445.
35. Jung, W., K. Sengupta, …, P. Chen. 2020. NAR breakthrough article biphasic unbinding of a metalloregulator from DNA for transcription (de)repression in live bacteria. *Nucleic Acids Res.* 48:2199–2208.
36. Dahlke, K., and C. E. Sing. 2017. Facilitated dissociation kinetics of dimeric nucleoid-associated proteins follow a universal curve. *Biophysical J.* 112:543–551.
37. Erbaş, A., M. O. de la Cruz, and J. F. Marko. 2018. Effects of electrostatic interactions on ligand dissociation kinetics. *Phys. Rev. E.* 97:022405.
38. Schneider, R., R. Lurz, …, G. Muskhelishvili. 2001. An architectural role of the *Escherichia coli* chromatin protein FIS in organising DNA. *Nucleic Acids Res.* 29:5107–5114.
39. Yildirim, A., and M. Feig. 2018. High-resolution 3D models of Caulobacter crescentus chromosome reveal genome structural variability and organization. *Nucleic Acids Res.* 46:3937–3952.
40. Dorier, J., and A. Stasiak. 2013. Modelling of crowded polymers elucidate effects of double-strand breaks in topological domains of bacterial chromosomes. *Nucleic Acids Res.* 41:6808–6815.

41. Jun, S., and B. Mulder. 2006. Entropy-driven spatial organization of highly confined polymers: lessons for the bacterial chromosome. *Proc. Natl. Acad. Sci. United States America.* 103:12388–12393.

42. Le Treut, G., F. Képès, and H. Orland. 2016. Phase behavior of DNA in the presence of DNA-binding proteins. *Biophysical J.* 110:51–62.

43. Brackley, C. A., S. Taylor, …, D. Marenduzzo. 2013. Nonspecific bridging-induced attraction drives clustering of DNA-binding proteins and genome organization. *Proc. Natl. Acad. Sci. U S A.* 110:E3605–E3611.

44. Kremer, K., and G. S. Grest. 1990. Dynamics of entangled linear polymer melts:FIXME A molecular-dynamics simulation. *J. Chem. Phys.* 92:5057–5086.

45. Grest, G. S., and M. Murat. 1993. Structure of grafted polymeric brushes in solvents of varying quality: a molecular dynamics study. *Macromolecules.* 26:3108–3117.

46. Hancock, S. P., S. Stella, …, R. C. Johnson. 2016. DNA sequence Determinants controlling affinity, stability and shape of DNA complexes bound by the nucleoid protein Fis. *PLoS One.* 11:e0150189.

47. Gao, Y., Y. H. Foo, …, L. J. Kenney. 2017. Charged residues in the H-NS linker drive DNA binding and gene silencing in single cells. *Proc. Natl. Acad. Sci. U S A.* 114:12560–12565.

48. Gawade, P., G. Gunjal, …, P. Ghosh. 2020. Reconstruction of transcriptional regulatory networks of Fis and H-NS in *Escherichia coli* from genome-wide data analysis. *Genomics.* 112:1264–1272. https://www.sciencedirect.com/science/article/pii/S0888754319302721.

49. Verma, S. C., Z. Qian, and S. L. Adhya. 2019. Architecture of the *Escherichia coli* nucleoid. *PLoS Genet.* 15:e1008456.

50. Tsai, M.-Y., B. Zhang, …, P. G. Wolynes. 2016. Molecular mechanism of facilitated dissociation of Fis protein from DNA. *J. Am. Chem. Soc.* 138:13497–13500.

51. Cocco, S., J. F. Marko, and R. Monasson. 2014. Stochastic ratchet mechanisms for replacement of proteins bound to DNA. *Phys. Rev. Lett.* 112:238101–238105.

52. Feldman-Cohen, L. S., Y. Shao, …, R. Osuna. 2006. Common and variable contributions of Fis residues to high-affinity binding at different DNA sequences. *J. Bacteriol.* 188:2081–2095.

53. Plimpton, S. 1995. Fast parallel algorithms for short-range molecular dynamics. *J. Comput. Phys.* 117:1–19. https://www.sciencedirect.com/science/article/pii/S002199918571039X.

54. Harris, C. R., K. J. Millman, …, T. E. Oliphant. 2020. Array programming with NumPy. *Nature.* 585:357–362. https://doi.org/10.1038/s41586-020-2649-2.

55. Humphrey, W., A. Dalke, and K. Schulten. 1996. VMD: visual molecular dynamics. *J. Mol. graphics.* 14:33–38.

56. Stukowski, A. 2010. Visualization and analysis of atomistic simulation data with OVITO-the Open Visualization Tool. *Model. Simulation Mater. Sci. Eng.* 18:015012.

57. Mazzocca, M., E. Colombo, …, D. Mazza. 2021. Transcription factor binding kinetics and transcriptional bursting: what do we really know? *Curr. Opin. Struct. Biol.* 71:239–248.

58. Shao, Y., L. S. Feldman-Cohen, and R. Osuna. 2008. Functional characterization of the *Escherichia coli* Fis–DNA binding sequence. *J. Mol. Biol.* 376:771–785.

59. Gupta, A., A. Wasim, and J. Mondal. 2020. Nucleoid associated proteins and their effect on *E. coli* chromosome. *bioRxiv*.

60. Lioy, V. S., A. Cournac, …, R. Koszul. 2018. Multiscale structuring of the *E. coli* chromosome by nucleoid-associated and condensin proteins. *Cell.* 172:771–783.e18.

61. Zhang, J., Y. Zeuner, …, A. Janshoff. 2004. Multiple site-specific binding of Fis protein to *Escherichia coli* nuoA-N promoter DNA and its impact on DNA topology visualised by means of scanning force microscopy. *Chembiochem : a Eur. J. Chem. Biol.* 5:1286–1289.

62. Parsaeian, A., M. O. de la Cruz, and J. F. Marko. 2013. Binding-rebinding dynamics of proteins interacting nonspecifically with a long DNA molecule. *Phys. Rev. E.* 88:675.

63. Hancock, S. P., T. Ghane, …, R. C. Johnson. 2013. Control of DNA minor groove width and Fis protein binding by the purine 2-amino group. *Nucleic Acids Res.* 41:6750–6760.

64. Halford, S. E., and J. F. Marko. 2004. How do site-specific DNA-binding proteins find their targets? *Nucleic Acids Res.* 32:3040–3052.

65. Stracy, M., J. Schweizer, …, C. Lesterlin. 2021. Transient non-specific DNA binding dominates the target search of bacterial DNA-binding proteins. *Mol. Cell.* 81:1499–1514.e6.

66. Azam, T. A., S. Hiraga, and A. Ishihama. 2000. Two types of localization of the DNA-binding proteins within the *Escherichia coli* nucleoid. *Genes Cell: devoted Mol. Cell. Mech.* 5:613–626.

67. Wang, W., G.-W. Li, …, X. Zhuang. 2011. Chromosome organization by a nucleoid-associated protein in live bacteria. *Science.* 333:1445–1449.

68. Japaridze, A., S. Renevey, …, G. Muskhelishvili. 2017. Spatial organization of DNA sequences directs the assembly of bacterial chromatin by a nucleoid-associated protein. *J. Biol. Chem.* 292:7607–7618.

69. Bétermier, M., D. J. Galas, and M. Chandler. 1994. Interaction of Fis protein with DNA: bending and specificity of binding. *Biochimie.* 76:958–967.

70. Pul, Ü., and R. Wagner. 2010. Nucleoid-Associated Proteins: Structural Properties. Springer Netherlands, Dordrecht, pp. 149–173.

71. Dorman, C. J. 2013. Genome architecture and global gene regulation in bacteria: making progress towards a unified model? *Nat. Rev. Microbiol.* 11:349–355.

72. Browning, D. F., D. C. Grainger, and S. J. W. Busby. 2010. Effects of nucleoid-associated proteins on bacterial chromosome structure and gene expression. *Curr. Opin. Microbiol.* 13:773–780.

73. Stracy, M., C. Lesterlin, …, A. N. Kapanidis. 2015. Live-cell superresolution microscopy reveals the organization of RNA polymerase in the bacterial nucleoid. *Proc. Natl. Acad. Sci. U S A.* 112:E4390–E4399.

74. Ross, W., J. F. Thompson, …, R. L. Gourse. 1990. E.coli Fis protein activates ribosomal RNA transcription *in vitro* and *in vivo*. *EMBO J.* 9:3733–3742.

75. Bradley, M. D., M. B. Beach, …, R. Osuna. 2007. Effects of Fis on *Escherichia coli* gene expression during different growth stages. *Microbiology.* 153:2922–2940.

76. Kahramanoglou, C., A. S. N. Seshasayee, …, N. M. Luscombe. 2010. Direct and indirect effects of H-NS and Fis on global gene expression control in *Escherichia coli*. *Nucleic Acids Res.* 39:2073–2091. https://doi.org/10.1093/nar/gkq934.

77. Garcia, D. A., G. Fettweis, …, G. L. Hager. 2021. Power-law behavior of transcription factor dynamics at the single-molecule level implies a continuum affinity model. *Nucleic Acids Res.* 49:6605–6620.

78. Gruszka, D. T., S. Xie, …, H. Yardimci. 2020. Single-molecule imaging reveals control of parental histone recycling by free histones during DNA replication. *Sci. Adv.* 6:eabc0330.